A New Role for Lipocalin Prostaglandin D Synthase in the Regulation of Brown Adipose Tissue Substrate Utilization

Sam Virtue,[1] Helena Feldmann,[2] Mark Christian,[3] Chong Yew Tan,[1] Mojgan Masoodi,[6] Martin Dale,[1] Chris Lelliott,[4] Keith Burling,[1] Mark Campbell,[1] Naomi Eguchi,[5] Peter Voshol,[1] Jaswinder K. Sethi,[1] Malcolm Parker,[3] Yoshihiro Urade,[5] Julian L. Griffin,[6] Barbara Cannon,[2] and Antonio Vidal-Puig[1]

In this study, we define a new role for lipocalin prostaglandin D synthase (L-PGDS) in the control of metabolic fuel utilization by brown adipose tissue (BAT). We demonstrate that *L-PGDS* expression in BAT is positively correlated with BAT activity, upregulated by peroxisome proliferator–activated receptor γ coactivator 1α or 1β and repressed by receptor-interacting protein 140. Under cold-acclimated conditions, mice lacking *L-PGDS* had elevated reliance on carbohydrate to provide fuel for thermogenesis and had increased expression of genes regulating glycolysis and de novo lipogenesis in BAT. These transcriptional differences were associated with increased lipid content in BAT and a BAT lipid composition enriched with de novo synthesized lipids. Consistent with the concept that lack of L-PGDS increases glucose utilization, mice lacking *L-PGDS* had improved glucose tolerance after high-fat feeding. The improved glucose tolerance appeared to be independent of changes in insulin sensitivity, as insulin levels during the glucose tolerance test and insulin, leptin, and adiponectin levels were unchanged. Moreover, *L-PGDS* knockout mice exhibited increased expression of genes involved in thermogenesis and increased norepinephrine-stimulated glucose uptake to BAT, suggesting that sympathetically mediated changes in glucose uptake may have improved glucose tolerance. Taken together, these results suggest that L-PGDS plays an important role in the regulation of glucose utilization in vivo. ***Diabetes*** **61:3139–3147, 2012**

Obesity is a chronic illness that is associated with multiple secondary diseases, including diabetes and cardiovascular disease. Although many ideas have been put forward to explain mechanistically how obesity leads to metabolic complications, this still remains an area of considerable controversy. We and others have suggested that alterations in how lipids are stored and handled may link obesity to metabolic complications through defects in adipose tissue expansion and functional capacity and the process of lipotoxicity (1,2).

From the [1]University of Cambridge Metabolic Research Laboratories, Institute of Metabolic Science, Addenbrooke's Treatment Centre, Addenbrooke's Hospital, Cambridge, U.K.; [2]Wenner-Gren Institute, University of Stockholm, Stockholm, Sweden; the [3]Molecular Endocrinology Laboratory, Institute of Reproductive and Developmental Biology, Imperial College London, London, U.K.; the [4]Department of Research and Development, AstraZeneca, Mölndal, Sweden; the [5]Osaka Bioscience Institute, Osaka, Japan; and [6]Human Nutrition Research and the Department of Biochemistry, Medical Research Council, Cambridge, U.K.

Corresponding authors: Sam Virtue, sv234@medschl.cam.ac.uk, and Antonio Vidal-Puig, ajv22@medschl.cam.ac.uk.

Received 5 January 2012 and accepted 13 June 2012.

DOI: 10.2337/db12-0015

This article contains Supplementary Data online at http://diabetes.diabetesjournals.org/lookup/suppl/doi:10.2337/db12-0015/-/DC1.

An important aspect of appropriate lipid handling is the ability of tissues to switch between carbohydrate and lipid as their major metabolic substrates. Under normal physiological conditions, humans switch from using high levels of carbohydrate during the postprandial state to predominantly utilizing stored lipids during the fasted state. The process of switching from fed to fasted states requires adipose tissue to play an important role in lipid buffering. During the fed state, net lipid flux into adipose tissue increases, whereas in the fasted state net lipid efflux predominates (3). Under pathological conditions where adipose tissue becomes insulin resistant, however, the appropriate fluxes into and out of adipose tissue are blunted (4–6).

The process of being able to switch between using metabolic substrates is termed *metabolic flexibility* and can be measured by assessing the change in respiratory quotient between fed and fasted states. A reduction in metabolic flexibility has been suggested to be a primary defect leading to insulin resistance. When fed a high-fat diet for 3 days, subjects with a family history of type 2 diabetes showed a lower change in respiratory quotient between fasted and fed states than did subjects without a family history of type 2 diabetes (7). The fact that impairments in metabolic substrate utilization may be a primary cause of insulin resistance suggests the possibility of a direct regulatory mechanism controlling this process; however, what form this mechanism takes is poorly understood.

In addition to the known roles for white adipose tissue (WAT) depots in metabolic health, interest in the role of brown adipose tissue (BAT) in adult humans has recently experienced a resurgence through studies with fluorodeoxyglucose positron emission tomography (8–13). BAT has been demonstrated, at least in rodents, to have a very high capacity for both lipid and glucose uptake and oxidation. In small mammals, such as mice, BAT may be responsible for the oxidation of as much as 90% of the total daily fuel intake. In addition to its high rate of lipid and glucose oxidation, BAT also has very high rates of de novo lipogenesis, suggested to account for as much as 40% of all de novo lipogenesis in a cold-exposed rats (14). Given BAT's very high metabolic rate, its high levels of lipid and glucose oxidation, and its substantial lipid synthesis, elucidation of how fuel utilization is regulated within BAT is an important question, particularly if it is ever to be used efficiently as a therapy to treat human metabolic disease. In this study we investigate the role of lipocalin prostaglandin D synthase (*L-PGDS*) in the regulation of carbohydrate and lipid utilization by BAT.

L-PGDS has at least two known functions. It is capable of synthesizing D-series prostaglandins, and it also can act as a carrier of lipophilic molecules (15). It has been

reported to have a protective role in the development of atherosclerosis (16). Reports regarding the role of L-PGDS in insulin sensitivity, however, are unclear. One report stated that lack of *L-PGDS* causes glucose intolerance, whereas a second report demonstrated that mice lacking *L-PGDS* had greater adiposity but unaltered glucose tolerance—suggesting that *L-PGDS* knockout (KO) mice may be disproportionately glucose tolerant for their degree of adiposity (16,17).

In this study we demonstrated that *L-PGDS* is highly regulated in BAT. To investigate a putative role for L-PGDS in BAT function, *L-PGDS* KO mice were cold acclimated. Cold acclimation causes a substantial increase in whole-organism metabolic rate and demands large alterations in carbohydrate and lipid metabolism, particularly in BAT. Mice lacking *L-PGDS* had lower basal metabolic rates, although they were still able to achieve the same maximal thermogenic capacity as wild-type mice. Crucially, *L-PGDS* KO mice had reduced lipid and increased carbohydrate utilization, appearing to meet increased demand for oxidative capacity from carbohydrate, either directly or by de novo synthesis of lipids and their subsequent oxidation, rather than from utilization of dietary lipids. Consistent with the concept that a lack of L-PGDS increases net glucose utilization, we showed that mice lacking *L-PGDS* had improved glucose tolerance when fed a high-fat diet. Overall, we have defined a role for L-PGDS in the control of fuel utilization by BAT.

RESEARCH DESIGN AND METHODS

Generation of mice. Mice heterozygous for a disruption in exons II–V in the *L-PGDS* gene were crossed to produce *L-PGDS* KO mice and wild-type controls (18,19). KO mice for the gene for peroxisome proliferator–activated receptor γ coactivator *PGC1β* were generated as previously described (20). KO mice for the *RIP140* were generated as previously described (21).

Animal care and diets. Mice were housed at a density of four animals per cage in a temperature-controlled room (20–22°C) with 12-h light/dark cycles. All animal protocols used in this study were approved by the U.K. Home Office and the University of Cambridge. Animals were fed a normal chow diet (D12450B; Research Diets) or a high-fat diet; either 45% or 60% calories-from-fat diets (D12451, D12492; Research Diets). For studies of cold acclimation, animals were housed as described previously (22). These experiments were approved by the North Stockholm Animal Ethics Committee.

Cell lines and plasmids. The brown fat cell line IMBAT-1 was generated (23) and differentiated, as described previously (24,25). The RIPKO-1 cell line was generated by continuous culture of Rip140-null mouse embryonic fibroblasts, and differentiation of the cells was performed as previously described (26). Differentiated IMBAT-1 or RIPKO-1 adipocytes were infected with adenovirus vectors expressing *Rip140*, *PGC1α*, or green fluorescent protein gene (26). Equal levels of infection were confirmed by fluorescence microscopy for the coexpressed green fluorescent protein.

Eicosanoid extraction and quantification. Eicosanoids were extracted from 50 to 100 mg of BAT by solid-phase extraction and quantified by liquid chromatography-mass spectrometry as described previously (27).

Hepatic glycogen assay. Glycogen levels were determined by the anthrone method (28).

Hepatic triglyceride analysis. Lipids were extracted from 100 mg of homogenized liver by heating to 85°C in 1 mL of 5% NP-40 in water. Triglyceride (TG) levels in extracts were assessed by enzymatic assay (Biovision) according to manufacturer instructions.

Blood biochemistry and body composition analysis. Enzymatic assay kits were used for determination of plasma free fatty acids (Roche) and TGs (Sigma-Aldrich, St. Louis, MO). Enzyme-linked immunosorbent assay kits were used for measurements of leptin (R & D Systems), insulin (DRG; Diagnostics International Limited), and adiponectin (B-Bridge International) according to manufacturer instructions. A Minispec LF TD-NMR (Brucker Optics) was used to measure body composition.

Fatty acid methyl ester analysis. The lipid extract was derivatized by acid-catalyzed esterification (29) with 10% BF_3 in methanol (Sigma-Aldrich, Gillingham, U.K.), and the esterification was performed at 80°C for 90 min. Once cool, water and hexane were added, and the aqueous layer was discarded. The organic layer was dried and then reconstituted in hexane for gas chromatography–flame ionization detection analysis (GC-FID) with a Trace GC Ultra (ThermoScientific). Derivatized organic samples were injected onto a 30-m × 0.25-mm 70% cyanopropyl polysilphenylene-siloxane 0.25 μm TR-FAME stationary-phase column (ThermoScientific). The initial column temperature was 55°C for 2 min, increased by 15°C/minute to 150°C and then increased at a rate of 4°C/minute to 230°C, where it was held for 30 s.

Norepinephrine-induced thermogenesis. Norepinephrine-induced thermogenesis was measured through oxygen consumption, as determined by the INCA system (Somedic, Hörby, Sweden) as described previously (30).

Glucose and pyruvate tolerance tests. Mice were fasted overnight from 4 P.M. until 9 A.M. the next day. Mice were injected intraperitoneally with either glucose (1 g/kg) or pyruvate (1.3 g/kg), and blood glucose levels were measured with a One-Touch Ultra glucose meter (Lifescan, Milpitas, CA). Blood samples for insulin measurement were collected with glass capillary tubes.

Histology. Samples for histology were placed in 10% buffered formalin overnight before transfer to 70% ethanol and later embedding in paraffin. Multiple sections were stained with hematoxylin and eosin for morphological analysis. Percentages of lipid content and adipocyte area were determined by morphometric analysis. The average lipid area in BAT and cell size in WAT per mouse were calculated from at least 3 separate sections. Analysis was carried out with CELL^P analysis software (Olympus, Southend-on-Sea, U.K.).

Quantitative real-time PCR. Total RNA was isolated from cells and BAT fractions with RNeasy Mini columns (Qiagen). RNA was isolated from ground tissues with STAT-60 reagent (TEL-TEST), followed by chloroform extraction and isopropanol precipitation. The cDNA was generated with M-MLV reverse transcriptase (Promega) according to the manufacturer instructions. Real-time PCR was carried out with TaqMan primers and probes or SYBR green reagent (Applied Biosystems) with an ABI Prism 7900 sequence detection system (Applied Biosystems) according to the manufacturer instructions. Data were normalized to 18s rRNA. Primer sequences are available on request.

Norepinephrine-stimulated glucose uptake. Mice were fasted overnight. Mice were subsequently anesthetized with 90 mg/kg sodium pentobarbital. After 10–15 min to allow full sedation, the tail vein was cannulated. A basal glucose sample was taken, and mice were injected with 0.2 MBq of 2-[^{14}C]-deoxyglucose (2-[^{14}C]-DG) (Perkin Elmer) and 1 mg/kg norepinephrine bistartrate. Glucose was measured at 10, 20, and 30 min with an AlphaTRAK (Abbott) glucose meter calibrated for rodents. Blood samples (30 μL) were collected at 10 and 20 min from the tail vein for measurement of serum DPM. At 30 min, animals were exsanguinated by cardiac puncture. Tissues were collected and frozen on dry ice. The 2-[^{14}C]-DG uptake into tissues was quantified with the $BaOH_2/ZnSO_4$ precipitation method as described previously (31).

Statistics. Results were expressed as mean ± SEM. Statistical analysis was performed with SPSS 17.0 (IBM, Armonk, NY). Pairwise comparisons were carried out by Student *t* test. For data with more than two groups, ANOVA was carried out, followed by Tukey post hoc test. For groups with multiple groups and conditions, two-way ANOVA was carried out.

RESULTS

Regulation of *L-PGDS* in BAT from states of altered thermogenesis. Two paradigms of BAT activation were investigated: *1*) cold exposure and *2*) high-fat feeding. *L-PGDS* expression was physiologically upregulated in the BAT of mice after either cold acclimation (4°C) or high-fat feeding (45% calories from fat) relative to chow-fed mice housed at room temperature (22°C) (Fig. 1*A*). Conversely, mice housed at thermoneutrality (30°C) for 3 weeks had decreased *L-PGDS* expression relative to room temperature–housed control mice (Fig. 1*B*). To identify putative transcriptional regulators of *L-PGDS*, we focused on key factors implicated in BAT activation. Both PGC1α and PGC1β have been shown to be positive regulators of BAT function, whereas RIP140 is a negative regulator of BAT function (20,32). *L-PGDS* was found to be down regulated in mice lacking *PGC1α* (Fig. 1*C*) or *PGC1β* (Fig. 1*E*) but upregulated in mice lacking *Rip140* (Fig. 1*D*). Finally, and consistent with a metabolic role for L-PGDS, *L-PGDS* was found to be predominantly expressed in mature brown adipocytes rather than the stromal vascular fraction (Fig. 1*F*).

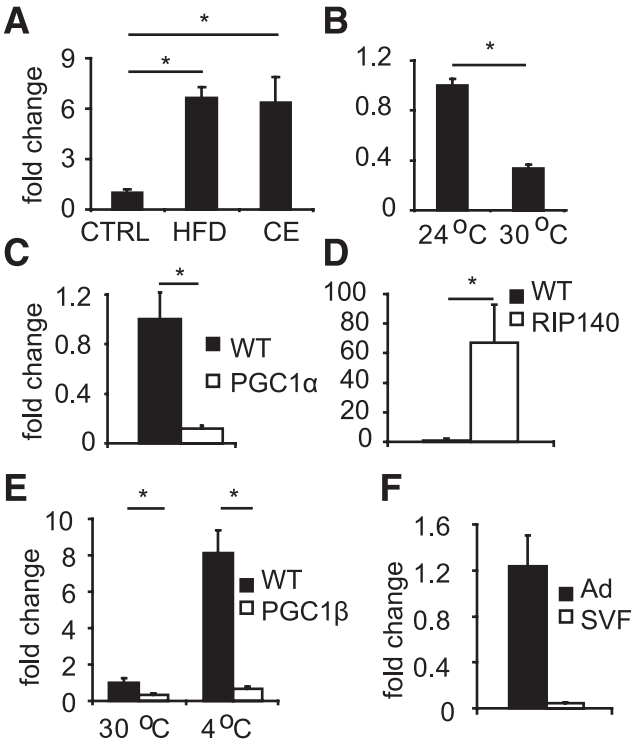

FIG. 1. *A*: *L-PGDS* mRNA is induced in active BAT, as shown in comparison of mice housed at 22°C fed a chow diet (CTRL); mice housed at 22°C fed a 45% calories-from-fat diet from weaning (HFD); and mice housed at 4°C for 3 weeks before tissue collection fed a chow diet (CE). All groups consisted of male mice $n > 7$ per group, C57Bl/6 background, 4 months old. *B*: *L-PGDS* mRNA levels are reduced in inactive BAT, as shown in comparison of mice housed for 3 weeks before tissue collection at either 22°C or 30°C fed a chow diet. Both groups consisted of female mice, $n > 7$ per group, mixed sv129/Bl6 background, 4 months old. *C*: *L-PGDS* mRNA levels in BAT are significantly lower in *PGC1α* KO mice compared with littermate controls (WT). Both groups consisted of male mice, $n = 8$ per group, C57Bl/6 background, 12 months old. *D*: Rip140 KO mice (RIP140) have significantly increased mRNA levels of *L-PGDS* in BAT relative WT. Both groups consisted of male mice, $n = 4$ per group, C57Bl/6 background, 4 months old. *E*: *L-PGDS* mRNA levels are significantly lower in *PGC1β* KO mice (*PGC1β*) compared with WT at both 30°C and 4°C. Both groups consisted of male mice, $n = 5$ per group, C57Bl/6 background, 4 months old. *F*: *L-PGDS* mRNA is expressed predominantly in mature adipocytes (Ad) relative to stromal vascular fraction (SVF). Both groups consisted of male mice, $n = 8$ per group, C57Bl/6 background, 4 months of age. Asterisks indicate $P < 0.05$.

Reciprocal regulation of *L-PGDS* by PGCs and RIP140 in vitro. To investigate further the reciprocal regulation of *L-PGDS* by PGCs and RIP140, cellular models were used. In a BAT cell line, ectopic overexpression of *PGC1α* caused an increase in endogenous *L-PGDS* mRNA levels (Fig. 2*A*). Conversely, increasing expression of Rip140 led to a decrease in *L-PGDS* expression levels (Fig. 2*B*). Finally, with *Rip140* KO embryonic fibroblasts, we showed that titrating RIP140 back into these cells resulted in a proportional decrease in *L-PGDS* expression (Fig. 2*C*).

L-PGDS regulates fuel utilization in vivo. To test whether L-PGDS was required for appropriate BAT function, *L-PGDS* KO mice were sequentially acclimated to either 4°C or thermoneutrality (30°C) for a period of 3 weeks. At each temperature, both basal and maximal thermogenic capacity were measured. *L-PGDS* KO mice exhibited no alterations in their norepinephrine-stimulated (maximal) rates of oxygen consumption; however, *L-PGDS* KO mice did exhibit a small reduction in their basal energy expenditure after housing at 4°C (Fig. 3*A*).

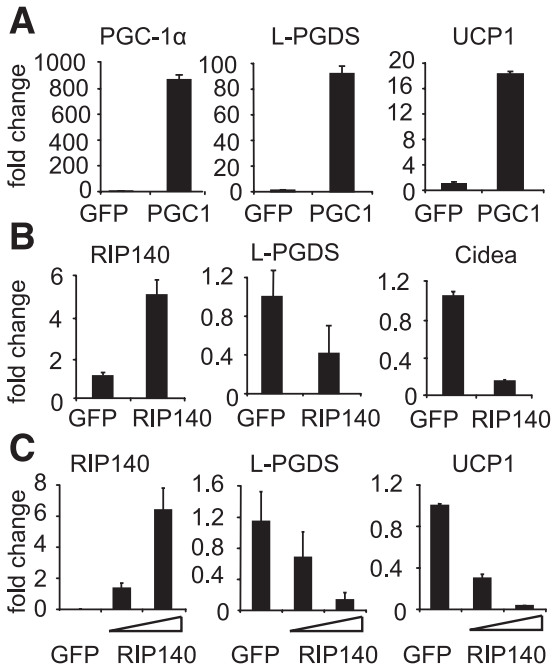

FIG. 2. *A*: *L-PGDS* mRNA levels are increased in an immortalized brown adipocyte cell line transfected with *PGC1α*. *B*: *L-PGDS* mRNA levels are suppressed in an immortalized brown adipocyte cell line transfected with *Rip40* (*RIP140*). *C*: *L-PGDS* mRNA levels are suppressed by RIP140 reexpression in mouse embryonic fibroblasts derived from *Rip140* KO mice in a dose-dependent manner. For all, $n = 3$ independent experiments.

Although changes in energy expenditure in *L-PGDS* KO mice were modest, there was a large alteration in their respiratory exchange ratio (RER) after norepinephrine stimulation at both 4°C and 30°C. Under unstimulated conditions, *L-PGDS* KO mice only exhibited an increase in RER when they had been previously acclimated to 4°C (Fig. 3*B*). The elevated RER of the *L-PGDS* KO mice relative to wild-type littermates suggests that *L-PGDS* KO mice met their increased demand for energy at 4°C by utilizing more carbohydrate than did wild-type mice.

Cold-acclimated *L-PGDS* KO mice exhibit altered lipid metabolism in BAT and liver. After cold acclimation, *L-PGDS* KO mice had increased lipid content in BAT relative to wild-type mice (Fig. 3*C*). Lipids were extracted from wild-type and *L-PGDS* KO mice that had been acclimated to 4°C for 3 weeks and were analyzed by GC-FID. The lipid profile of the *L-PGDS* KO mice, when compared with wild-type controls, demonstrated a reduction in the proportion of dietary-derived essential fatty acids (C18:2 and C18:3), and an increase in the proportion of oleate (C18:1), which can be either derived from the diet or synthesized de novo (Fig. 3*D*). In accordance with elevated de novo lipogenesis, BAT from *L-PGDS* KO mice also had increased expression of the lipogenic genes for fatty acid synthase (*FAS*), stearoyl coenzyme A desaturase 1 (*Scd1*), and elongase 6 (*Elovl6*) (Fig. 4*A*). When compared with wild-type mice, *L-PGDS* KO mice had increased mRNA levels in BAT of the glucose transporter gene *Glut4*, α-enolase, and phosphofructokinase, genes involved in glucose uptake and glycolysis (Fig. 4*B*). Remarkably, the gene expression changes in both carbohydrate metabolism and fatty acid synthesis were highly specific. Although there was a small increase in UCP1 expression in BAT,

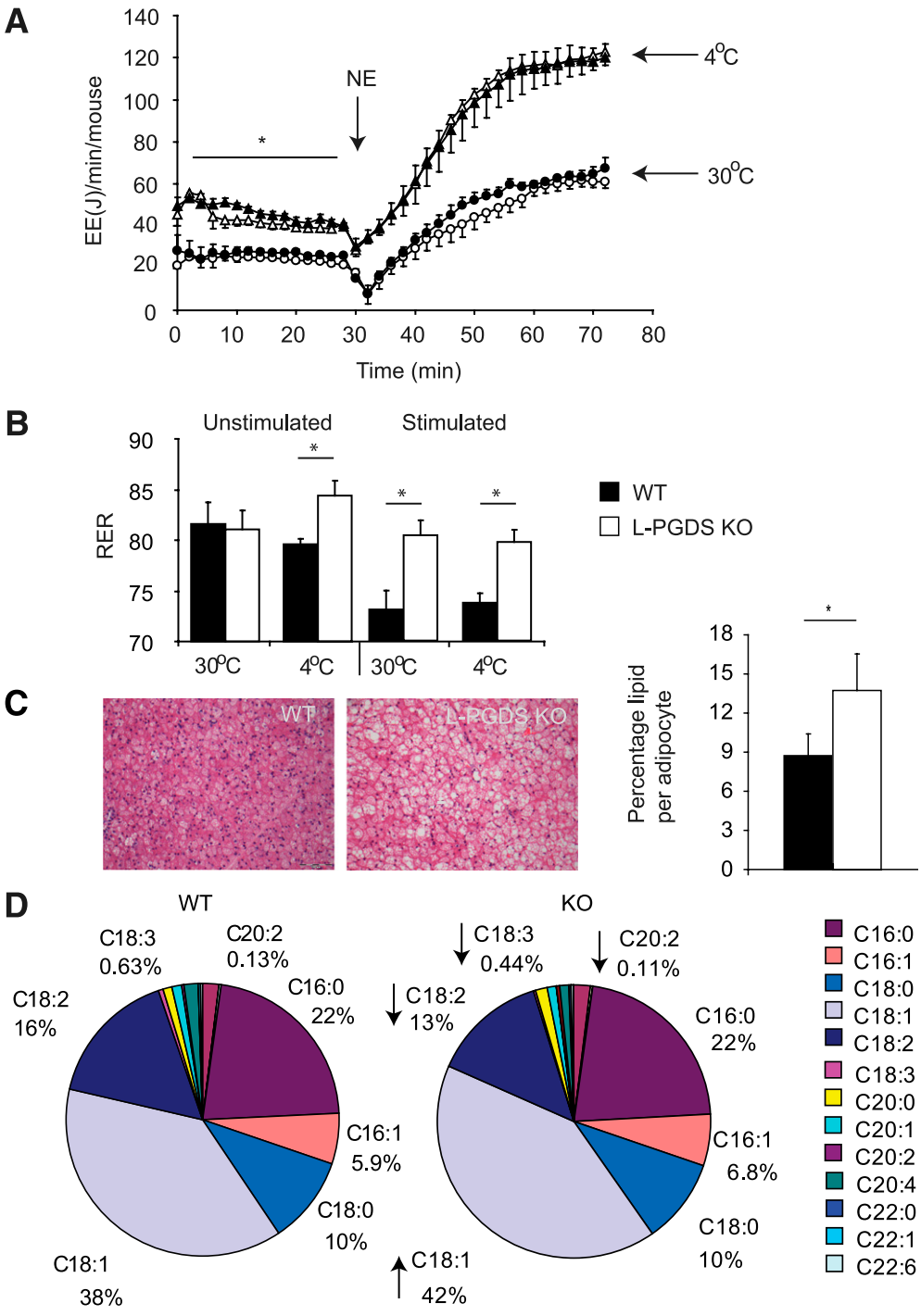

FIG. 3. ***A*****: *L-PGDS* KO mice have no difference in maximal norepinephrine-stimulated (*NE*) oxygen consumption after acclimation to either 4°C or 30°C but demonstrate a reduction in basal energy expenditure (EE) after acclimation to 4°C. Maximal oxygen consumption was analyzed by injecting anesthetized mice with norepinephrine. All measurements were conducted at 33°C regardless of previous acclimation temperature. Solid triangles, WT mice acclimated to 4°C; open triangles, KO mice acclimated to 4°C; solid circles, WT mice acclimated to 30°C; open circles, KO mice acclimated to 30°C. *B*: Under basal conditions, *L-PGDS* KO mice (*L-PGDS KO*) have an increased RER compared with wild-type controls (WT) after housing at 4°C but not after housing at 30°C. After stimulation with norepinephrine, *L-PGDS* KO mice have an increased RER compared with wild-type mice regardless of previous housing. *C*: Representative histological sections of BAT from WT and *L-PGDS* KO mice housed at 4°C (*left*) and morphometric analysis of histology quantified for lipid droplet area per brown adipocyte (*right*) in *L-PGDS* KO mice (white bars) and WT controls (black bars). Both groups consisted of male mice, $n > 5$ per group, C57Bl/6, 7 months old. *D*: Analysis of fatty acid methyl esters by GC-FID analysis shows an increased level of de novo synthesized lipids and reduced levels of dietary essential fatty acids in BAT of *L-PGDS* KO mice relative to WT mice. Both groups consisted of male mice, $n = 8$ per group, C57Bl/6 background, 7 months old. *$P < 0.05$. (A high-quality digital representation of this figure is available in the online issue.)**

there were no significant changes observed in genes regulating brown adipocyte function, fatty acid oxidation, lipid uptake, or brown adipocyte differentiation (Fig. 4*C* and Supplementary Fig. 1). Taken together, these data suggest that *L-PGDS* ablation results in active BAT that preferentially utilizes glucose, either directly as a substrate for thermogenesis or for de novo lipogenesis and subsequent β-oxidation.

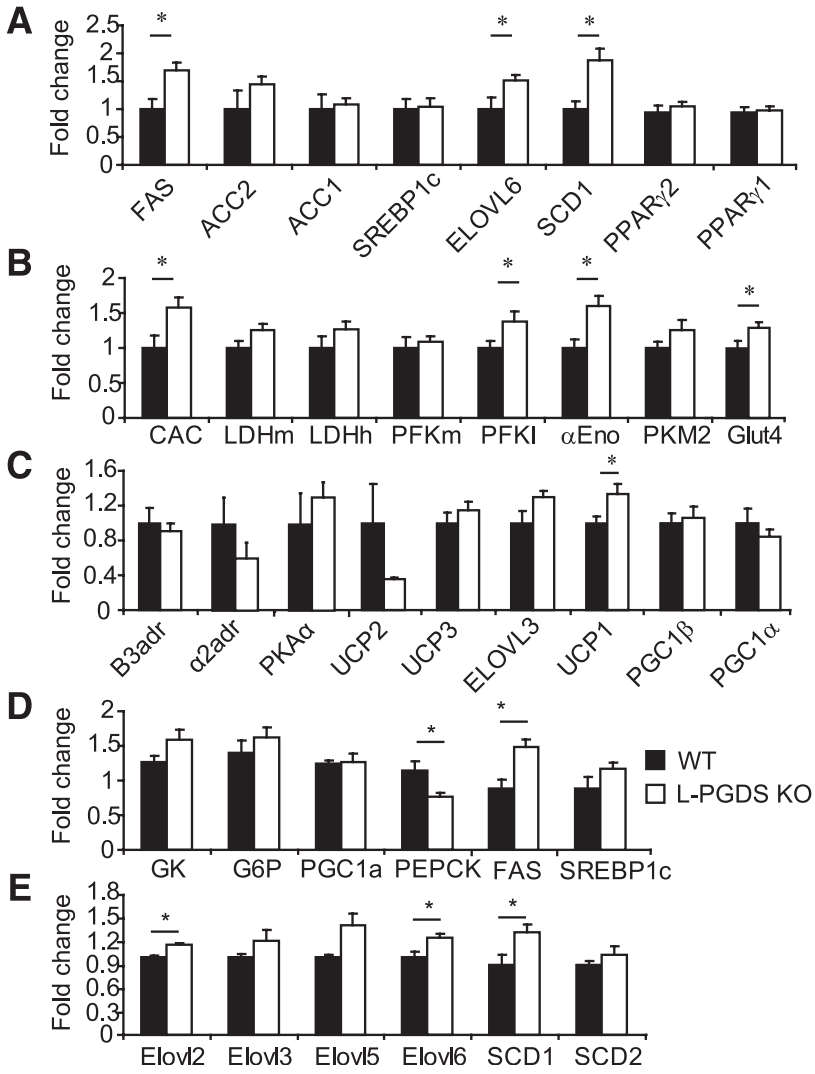

FIG. 4. Gene expression analysis by real-time PCR from BAT (*A–C*) and liver (*D* and *E*) of *L-PGDS* KO mice and controls (WT). In BAT, genes examined are involved in fatty acid synthesis (*A*), glucose metabolism (*B*), and uncoupling proteins and markers of thermogenesis (*C*). In liver, genes examined are involved in glucose and fatty acid metabolism (*D*) and fatty acid elongation and desaturation (*E*). Both groups consist of male mice, $n > 5$ per group, C57Bl/6 background, 7 months old, acclimated to 5°C for 3 weeks. *$P < 0.05$.

Similar to the results observed in BAT, *L-PGDS* KO mice had increased levels of *FAS*, *Elovl6*, and *Scd1* mRNA expression in liver when compared with wild-type mice (Fig. 4*D–E*). Despite these changes, no increase in hepatic TG level was detected (Supplementary Fig. 2*A*). Further to the changes in de novo lipogenesis, *L-PGDS* KO mice also exhibited a reduction in expression of the key gluconeogenic enzyme *PEPCK* (Fig. 4*D*), although no alterations in the glycogen biosynthetic program or glycogen levels were detected (Supplementary Fig. 2*B–C*). The change in *PEPCK* suggests that in the liver, products of the citric acid cycle were not driven toward production of glucose but instead were channeled to de novo lipogenesis. This hypothesis was also supported by the lower plasma glucose of cold-acclimated *L-PGDS* KO mice (Table 1) and by a small but significant reduction in glucose levels in response to a pyruvate tolerance test (Supplementary Fig. 2*D*).

L-PGDS–dependent alterations in lipid metabolism are organ specific. The major sites of de novo lipogenesis in cold-acclimated mice are BAT and liver (14). Consistent with L-PGDS acting principally to regulate fuel availability to and utilization by thermogenic tissues, comparatively few changes in gene expression were found in muscle (Supplementary Fig. 1*B–D*), epididymal WAT, or subcutaneous WAT (Supplementary Fig. 3). Overall, under conditions of cold exposure, loss of *L-PGDS* appeared almost exclusively to affect BAT depots and liver, which in the cold acts as an important supplier of de novo synthesized lipids for oxidation by BAT.

***L-PGDS* ablation increases glucose tolerance.** Given that our data had indicated that loss of L-PGDS in cold-acclimated animals appeared to increase glucose utilization to meet energy demands, we next investigated whether a lack of *L-PGDS* could affect lipid and carbohydrate metabolism under standard laboratory conditions (24°C housing). In animals fed a high-fat diet, lack of *L-PGDS* caused a significant improvement in glucose tolerance (Fig. 5*A*). Surprisingly, this effect was observed despite apparently similar degrees of insulin resistance induced by high-fat diet in WT and L-PGDS KO mice, as indicated by markers of insulin sensitivity including serum insulin levels during the glucose tolerance test (Fig. 5*B* and Supplementary Fig. 4*G*); adiposity (Fig. 5*C*); adipocyte size (Supplementary Fig. 4*A*); markers of adipogenesis in BAT,

TABLE 1
Serum biochemistry of WT and *L-PGDS* KO mice after cold acclimation

	Wild-type	*L-PGDS* KO	*P* value
Insulin (μg/L)	1.69 ± 0.36	1.51 ± 0.32	0.736
Glucose (mmol/L)	16.94 ± 1.67	13.21 ± 0.45	**0.045**
FFA (μmol/L)	555 ± 109	572.6 ± 31.4	0.876
TG (mmol/L)	1.54 ± 0.27	1.7 ± 0.128	0.593
Cholesterol (mmol/L)	3.14 ± 0.39	2.866 ± 0.088	0.481
HDL (mmol/L)	1.92 ± 0.15	1.818 ± 0.053	0.518
Adiponectin (ng/mL)	18,889 ± 1911	17,885 ± 646	0.611
Leptin (pg/mL)	6,642 ± 1933	5,191 ± 711	0.473

Data are mean ± SEM for male mice, $n > 5$ per group, C57/Bl6 background, 7 months old. Bold type indicates significant differences between groups. FFA, free fatty acid.

subcutaneous WAT, and epididymal WAT (Supplementary Fig. 4*B–D*), tissue weights (Supplementary Fig. 4*E–F*); and fasted insulin, adiponectin, and leptin levels (Fig. 5*E*). Tissue markers of insulin sensitivity were also unchanged between wild-type and *L-PGDS* KO mice (Supplementary Fig. 5). Consistent with increased glucose utilization, mice lacking *L-PGDS* had lower fasting glucose levels (Fig. 5*D*). Because the changes in glucose tolerance and fasting glucose did not seem to be associated with markers of improved insulin sensitivity, we investigated whether there were any changes in other processes that mediate glucose uptake. In BAT norepinephrine has been shown to promote glucose uptake independently of insulin (33). Consistent with increased sympathetic tone or sensitivity to sympathetic tone, mice lacking *L-PGDS* had elevated thermogenic markers in BAT, and the constitutive glucose transporter gene *Glut1* was also upregulated (Fig. 5*F*). To test whether response to sympathetic tone in terms of plasma glucose levels could be modulated by L-PGDS, we injected wild-type and *L-PGDS* KO mice with norepinephrine (1 mg/kg). As expected norepinephrine increased serum glucose levels as a result of its effects on hepatic glucose production (34,35); however, in *L-PGDS* KO mice the increase in plasma glucose levels was blunted relative to that in wild-type animals (Fig. 5*G*). To determine whether this was due to changes in glucose uptake as opposed to hepatic glucose uptake, we subsequently included 2-[^{14}C]-DG as a tracer to measure tissue-specific glucose uptake. We detected elevated uptake of glucose into BAT in response to norepinephrine, with no changes in muscle and a tendency ($P = 0.059$) toward increased glucose disposal into WAT. Although hepatic glucose production could not be directly assessed in the same assay, the elevated accumulation of 2-deoxy-D-glucose in liver in *L-PGDS* KO mice was suggestive of decreased glucose output, because 2-deoxy-D-glucose accumulates in liver by mass action (through *Glut2*) but can be actively exported.

Loss of *L-PGDS* does not affect prostaglandin D_2 levels in BAT. Finally, to try to identify a mechanism for L-PGDS in the regulation of fuel utilization, we measured prostaglandin D_2 and E_2 in BAT from cold acclimated wild-type and *L-PGDS* KO mice (Fig. 5*I*). We detected no differences in prostaglandin levels, suggesting that L-PGDS may act as a lipocalin.

DISCUSSION

In this study, we demonstrated that L-PGDS contributes to the balance between carbohydrate and lipid utilization in vivo. We also demonstrated that the physiological levels of *L-PGDS* mRNA in BAT are strongly and positively correlated with activation of BAT metabolism. In vivo characterization of cold-exposed mice lacking *L-PGDS* demonstrated that lack of *L-PGDS* resulted in a modest impairment in metabolic rate but a substantial increase in RER. These changes in metabolic rate and RER suggested that the principal role of L-PGDS was to control the type of fuel utilized by BAT, rather than the maximal thermogenic capacity.

The first evidence for a role for L-PGDS in BAT metabolism came from its dynamic regulation in response to both physiological and genetic manipulations which affect BAT function. *L-PGDS* mRNA was upregulated in states of elevated BAT function, including cold acclimation and high-fat feeding, as well as in the *Rip140* KO mouse model, which has substantially increased metabolic rate with elevated markers of brown adipocyte genes within WAT (32). Conversely, *L-PGDS* mRNA was downregulated by thermoneutral housing and in mouse models with reduced BAT function, including *PGC1α* and *PGC1β* KO mice. Notably, both *Rip140* KO and *PGC1β* KO mice have RER values that inversely correlate with their *L-PGDS* levels (20,36), consistent with the elevated RER seen in *L-PGDS* KO mice.

Although differences in metabolic rate observed between *L-PGDS* KO mice and wild-type controls were modest, there were much more substantial changes in RER. An elevated RER would usually be considered a marker of increased carbohydrate utilization and decreased lipid utilization by an organism; however, conversion of carbohydrate to lipid and its subsequent oxidation has the same RER as oxidizing carbohydrate itself, suggesting that either increased direct metabolism of carbohydrate or increased de novo lipogenesis followed by fatty acid oxidation could explain the differences in RER between wild-type and KO mice. In agreement with this, molecular analysis of BAT from *L-PGDS* KO mice demonstrated an increase in the proportion of de novo synthesized lipid located within BAT, as well as increased expression of glycolytic and de novo lipogenic enzymes, when compared with wild-type controls. Under conditions of cold acclimation, the principal sites of de novo lipogenesis are BAT and liver (14). Similarly to BAT, the livers of *L-PGDS* KO mice also exhibited a gene expression profile consistent with converting carbohydrate to lipid but did not exhibit any increase in hepatic TG levels, suggesting that any increased TG synthesis was potentially being exported. The molecular prolipogenic changes in liver and BAT were supported by lower serum glucose levels. Overall, these data suggest that under conditions of 4°C housing, L-PGDS is required for appropriate utilization of dietary lipids. In the absence of L-PGDS, mice were still able to meet the thermogenic demands of cold exposure; however, this appeared to be at the expense of a substantial increase in carbohydrate utilization.

In addition to cold exposure, high-fat feeding has been shown to promote BAT activation. After feeding with a very high-fat diet (60% calories from fat), *L-PGDS* KO mice had improved glucose tolerance relative to wild-type mice. Although euglycemic-hyperinsulinemic clamp data would be needed to formally confirm an absence of alterations in insulin sensitivity, there were no molecular markers of insulin resistance that differed between WT and *L-PGDS* KO mice, suggesting that the improved glucose tolerance of the *L-PGDS* KO mice could be driven by mechanisms not insulin dependent. Consistent with this concept, the thermogenic program in BAT and the

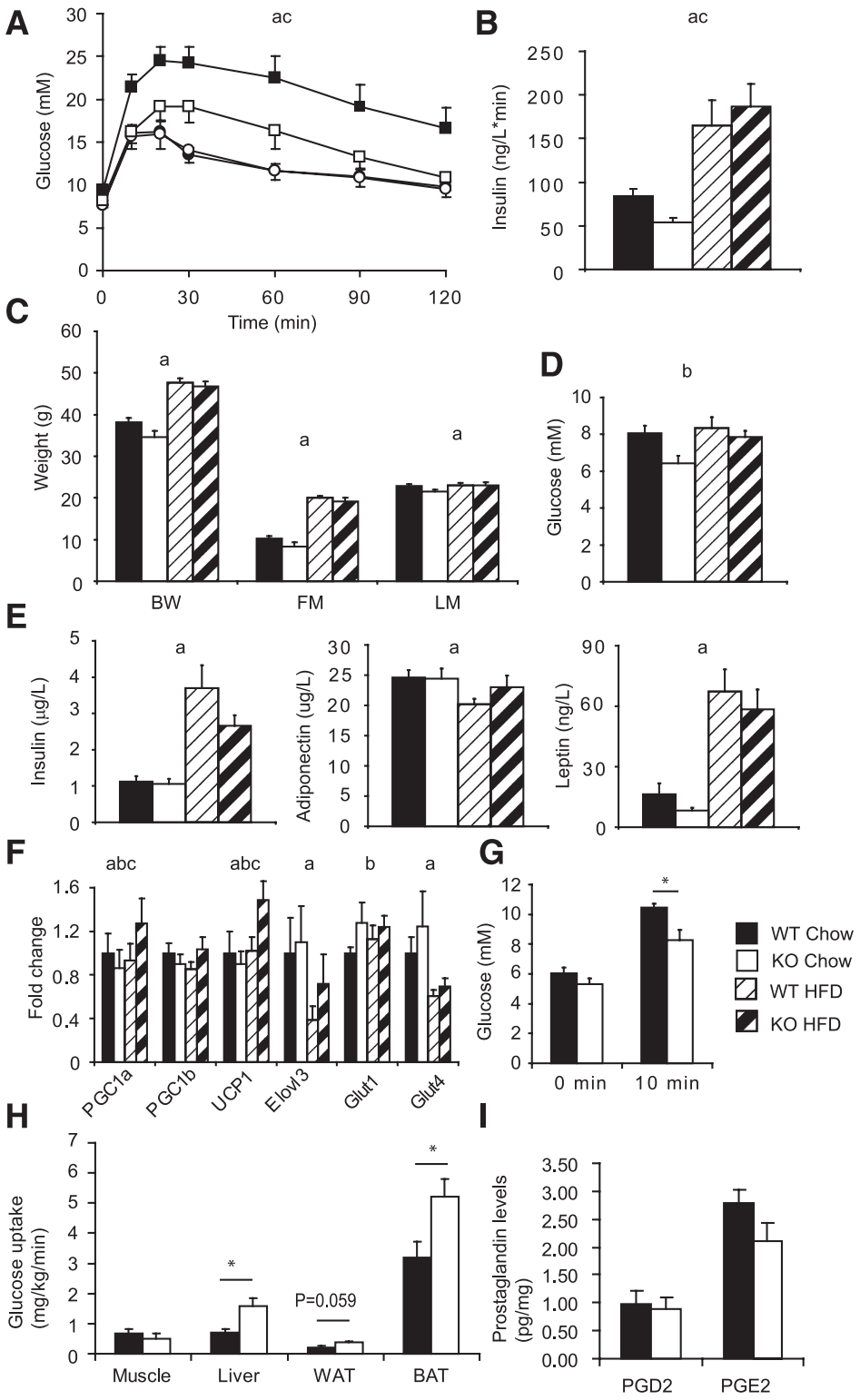

FIG. 5. ***A*: Glucose levels during an intraperitoneal glucose tolerance test in wild-type control (WT) mice fed chow (*black circles*), *L-PGDS* KO mice fed chow (*white circles*), WT mice fed a high-fat diet (*black squares*), and *L-PGDS* KO mice fed a high-fat diet. *B–I*: Area under the curve for insulin levels during glucose tolerance test (*B*); body weight (BW), fat mass (FM), and lean mass (LM) (*C*); fasting blood glucose levels (*D*); fasting serum hormone levels (*E*); gene expressions in intrascapular BAT (*F*); glucose levels in response to subcutaneous injection of norepinephrine (1 mg/kg) (*G*); tissue-specific glucose uptake in response to subcutaneous injection of norepinephrine (1 mg/kg) (*H*); and prostaglandin levels from BAT of cold-acclimated *WT* and *L-PGDS* KO mice (I). All animals were 7-month-old C57Bl/6 males, fed either chow or 60% calories-from-fat diet (HFD), $n = 8$ per group, fasted animals (except in *H* and *I*), $n = 7$ per group. *a*, $P < 0.05$ for diet; *b*, $P < 0.05$ for genotype; *c*, $P < 0.05$ for genotype and diet interaction. *$P < 0.05$.**

constitutive glucose transporter *Glut1* were upregulated in mice lacking *L-PGDS*. To test the concept that the sympathetic nervous system could regulate glucose levels in *L-PGDS* KO mice, we injected mice lacking *L-PGDS* with norepinephrine in combination with 2-[^{14}C]DG. Mice lacking *L-PGDS* exhibited a 60% increase in glucose disposal to BAT relative to wild-type controls, supporting the concept of sympathetically mediated glucose uptake into BAT being elevated in the absence of *L-PGDS*. BAT exhibits very high rates of glucose uptake in response to either norepinephrine or insulin, and although the exact contribution of glucose as a substrate for thermogenesis remains debatable, it seems likely that it does contribute significantly (37). Several publications have demonstrated sympathetic control of glucose uptake into BAT (38–42) and that this uptake is dependent on UCP1 (39). Insulin stimulated uptake of glucose to BAT is not dependent on it being thermogenically functional (40); however, cold exposure does increase the rate of glucose disposal into BAT in response to insulin (42). Overall, these results suggest that BAT can have a major impact on systemic glucose levels and, importantly, that it can do so independent of the actions of insulin.

The finding that L-PGDS can mediate fuel provision to BAT is a potentially important one given the renewed excitement in the potential of BAT to treat metabolic disease after its rediscovery in adult humans (8,12,43). Although much research into BAT has focused on its recruitment and molecular activation, relatively less research has gone into the supply of nutrients to BAT. Recent articles regarding angiogenesis in BAT (44) and the control of lipid uptake into BAT (45) have helped to further our understanding of fuel supply to BAT; however, if BAT is ever to be used to treat human obesity, then it must be both fully activated and appropriately supplied with nutrients. The ability of L-PGDS to control in part the balance of lipid and carbohydrate utilization by BAT highlights another potential layer of regulation of BAT activity.

To try to address in part how L-PGDS may affect BAT function on a molecular level, we measured prostaglandin levels in cold-acclimated BAT and detected no differences. Because L-PGDS is a bifunctional molecule capable of acting both as a carrier of lipophilic molecules (46) and as a prostaglandin synthase (15), the absence of changes in prostaglandins suggested that L-PGDS may act primarily as a lipocalin in terms of its regulatory role in BAT. What L-PGDS binds to and how that molecule may regulate BAT function will be an area for future study.

In summary, L-PGDS appears to regulate the balance between carbohydrate and lipid metabolism in BAT. The association between metabolic health and an ability to switch between carbohydrate and lipid metabolism is already established; however, the ability of L-PGDS to control the balance between lipid and carbohydrate utilization, with only minor effects on metabolic rate, highlights a new type of control mechanism for whole organism substrate handling that could potentially be used to bypass states of nutritionally induced or genetic insulin resistance.

ACKNOWLEDGMENTS

Diabetes U.K., EU HEPADIP FP6, The Medical Research Council Centre for Obesity Related Disorders, and the Medical Research Council funded this work. Studies in Stockholm were supported by the Swedish Research Council and ADAPT FP7 and the BBSRC.

C.L. is employed by AstraZeneca, Mölndal, Sweden. No other potential conflicts of interest relevant to this article were reported.

S.V., H.F., M.Ch., M.Ca., M.D., C.L., M.M., P.V., and K.B. performed experiments. S.V., C.Y.T., M.M., J.L.G., H.F., and B.C. analyzed data. S.V., M.P., P.V., J.K.S., J.L.G., B.C., and A.V.-P. designed experiments. S.V. and A.V.-P. wrote the manuscript. Y.U. and N.E. provided essential reagents. S.V. and A.V.-P. are the guarantors of this work and, as such, had full access to all of the data in the study and take responsibility for the integrity of the data and the accuracy of the data analysis.

The authors thank Helen Westby, Dan Hart, Agnes Lukasik, Sylvia Osborne, and Sarah Grocott, all from the University of Cambridge, for technical assistance.

REFERENCES

1. Virtue S, Vidal-Puig A. It's not how fat you are, it's what you do with it that counts. PLoS Biol 2008;6:e237
2. Virtue S, Vidal-Puig A. Adipose tissue expandability, lipotoxicity and the Metabolic Syndrome–an allostatic perspective. Biochim Biophys Acta 2010;1801:338–349
3. Frayn KN. Adipose tissue as a buffer for daily lipid flux. Diabetologia 2002; 45:1201–1210
4. Basu A, Basu R, Shah P, Vella A, Rizza RA, Jensen MD. Systemic and regional free fatty acid metabolism in type 2 diabetes. Am J Physiol Endocrinol Metab 2001;280:E1000–E1006
5. Martin ML, Jensen MD. Effects of body fat distribution on regional lipolysis in obesity. J Clin Invest 1991;88:609–613
6. McQuaid SE, Hodson L, Neville MJ, et al. Downregulation of adipose tissue fatty acid trafficking in obesity: a driver for ectopic fat deposition? Diabetes 2011;60:47–55
7. Ukropcova B, Sereda O, de Jonge L, et al. Family history of diabetes links impaired substrate switching and reduced mitochondrial content in skeletal muscle. Diabetes 2007;56:720–727
8. Cypess AM, Lehman S, Williams G, et al. Identification and importance of brown adipose tissue in adult humans. N Engl J Med 2009;360:1509–1517
9. Nedergaard J, Bengtsson T, Cannon B. Three years with adult human brown adipose tissue. Ann N Y Acad Sci 2010;1212:E20–E36
10. Ouellet V, Routhier-Labadie A, Bellemare W, et al. Outdoor temperature, age, sex, body mass index, and diabetic status determine the prevalence, mass, and glucose-uptake activity of ^{18}F-FDG-detected BAT in humans. J Clin Endocrinol Metab 2011;96:192–199
11. Saito M, Okamatsu-Ogura Y, Matsushita M, et al. High incidence of metabolically active brown adipose tissue in healthy adult humans: effects of cold exposure and adiposity. Diabetes 2009;58:1526–1531
12. van Marken Lichtenbelt WD, Vanhommerig JW, Smulders NM, et al. Cold-activated brown adipose tissue in healthy men. N Engl J Med 2009;360: 1500–1508
13. Zingaretti MC, Crosta F, Vitali A, et al. The presence of UCP1 demonstrates that metabolically active adipose tissue in the neck of adult humans truly represents brown adipose tissue. FASEB J 2009;23:3113–3120
14. Trayhurn P. Fatty acid synthesis in vivo in brown adipose tissue, liver and white adipose tissue of the cold-acclimated rat. FEBS Lett 1979;104: 13–16
15. Urade Y, Eguchi N. Lipocalin-type and hematopoietic prostaglandin D synthases as a novel example of functional convergence. Prostaglandins Other Lipid Mediat 2002;68-69:375–382
16. Tanaka R, Miwa Y, Mou K, et al. Knockout of the l-pgds gene aggravates obesity and atherosclerosis in mice. Biochem Biophys Res Commun 2009; 378:851–856
17. Ragolia L, Palaia T, Hall CE, Maesaka JK, Eguchi N, Urade Y. Accelerated glucose intolerance, nephropathy, and atherosclerosis in prostaglandin D2 synthase knock-out mice. J Biol Chem 2005;280:29946–29955
18. Eguchi N, Minami T, Shirafuji N, et al. Lack of tactile pain (allodynia) in lipocalin-type prostaglandin D synthase-deficient mice. Proc Natl Acad Sci USA 1999;96:726–730
19. Medina-Gomez G, Gray SL, Yetukuri L, et al. PPAR gamma 2 prevents lipotoxicity by controlling adipose tissue expandability and peripheral lipid metabolism. PLoS Genet 2007;3:e64
20. Lelliott CJ, Medina-Gomez G, Petrovic N, et al. Ablation of PGC-1beta results in defective mitochondrial activity, thermogenesis, hepatic function, and cardiac performance. PLoS Biol 2006;4:e369

21. White R, Leonardsson G, Rosewell I, Ann Jacobs M, Milligan S, Parker M. The nuclear receptor co-repressor nrip1 (RIP140) is essential for female fertility. Nat Med 2000;6:1368–1374
22. Golozoubova V, Cannon B, Nedergaard J. UCP1 is essential for adaptive adrenergic nonshivering thermogenesis. Am J Physiol Endocrinol Metab 2006;291:E350–E357
23. Jat PS, Noble MD, Ataliotis P, et al. Direct derivation of conditionally immortal cell lines from an H-2Kb-tsA58 transgenic mouse. Proc Natl Acad Sci USA 1991;88:5096–5100
24. Debevec D, Christian M, Morganstein D, et al. Receptor interacting protein 140 regulates expression of uncoupling protein 1 in adipocytes through specific peroxisome proliferator activated receptor isoforms and estrogen-related receptor alpha. Mol Endocrinol 2007;21:1581–1592
25. Hallberg M, Morganstein DL, Kiskinis E, et al. A functional interaction between RIP140 and PGC-1alpha regulates the expression of the lipid droplet protein CIDEA. Mol Cell Biol 2008;28:6785–6795
26. Christian M, Kiskinis E, Debevec D, Leonardsson G, White R, Parker MG. RIP140-targeted repression of gene expression in adipocytes. Mol Cell Biol 2005;25:9383–9391
27. Masoodi M, Nicolaou A, Gledhill K, Rhodes LE, Tobin DJ, Thody AJ. Prostaglandin D production in FM55 melanoma cells is regulated by alpha-melanocyte-stimulating hormone and is not related to melanin production. Exp Dermatol 2010;19:751–753
28. Roe JH, Dailey RE. Determination of glycogen with the anthrone reagent. Anal Biochem 1966;15:245–250
29. Morrison WR, Smith LM. Preparation of fatty acid methyl esters and dimethylacetals from lipids with boron fluoride–methanol. J Lipid Res 1964; 5:600–608
30. Alberts P, Johansson BG, McArthur RA. Characterization of energy expenditure in rodents by indirect calorimetry. Curr Protoc Neurosci 2006; Chapter 9:Unit9.23D
31. Tabas I, Kovanen PT. In search of an endpoint. Curr Opin Lipidol 2000;11: 447–450
32. Leonardsson G, Steel JH, Christian M, et al. Nuclear receptor corepressor RIP140 regulates fat accumulation. Proc Natl Acad Sci USA 2004;101:8437–8442
33. Liu X, Pérusse F, Bukowiecki LJ. Chronic norepinephrine infusion stimulates glucose uptake in white and brown adipose tissues. Am J Physiol 1994;266:R914–R920
34. Chu CA, Sindelar DK, Neal DW, Allen EJ, Donahue EP, Cherrington AD. Comparison of the direct and indirect effects of epinephrine on hepatic glucose production. J Clin Invest 1997;99:1044–1056
35. Stevenson RW, Steiner KE, Connolly CC, et al. Dose-related effects of epinephrine on glucose production in conscious dogs. Am J Physiol 1991; 260:E363–E370
36. Seth A, Steel JH, Nichol D, et al. The transcriptional corepressor RIP140 regulates oxidative metabolism in skeletal muscle. Cell Metab 2007;6:236–245
37. Cannon B, Nedergaard J. Metabolic consequences of the presence or absence of the thermogenic capacity of brown adipose tissue in mice (and probably in humans). Int J Obes (Lond) 2010;34(Suppl. 1):S7–S16
38. Gasparetti AL, de Souza CT, Pereira-da-Silva M, et al. Cold exposure induces tissue-specific modulation of the insulin-signalling pathway in *Rattus norvegicus*. J Physiol 2003;552:149–162
39. Inokuma K, Ogura-Okamatsu Y, Toda C, Kimura K, Yamashita H, Saito M. Uncoupling protein 1 is necessary for norepinephrine-induced glucose utilization in brown adipose tissue. Diabetes 2005;54:1385–1391
40. Shimizu Y, Nikami H, Saito M. Sympathetic activation of glucose utilization in brown adipose tissue in rats. J Biochem 1991;110:688–692
41. Vallerand AL, Lupien J, Bukowiecki LJ. Interactions of cold exposure and starvation on glucose tolerance and insulin response. Am J Physiol 1983; 245:E575–E581
42. Vallerand AL, Pérusse F, Bukowiecki LJ. Stimulatory effects of cold exposure and cold acclimation on glucose uptake in rat peripheral tissues. Am J Physiol 1990;259:R1043–R1049
43. Virtanen KA, Lidell ME, Orava J, et al. Functional brown adipose tissue in healthy adults. N Engl J Med 2009;360:1518–1525
44. Xue Y, Petrovic N, Cao R, et al. Hypoxia-independent angiogenesis in adipose tissues during cold acclimation. Cell Metab 2009;9:99–109
45. Bartelt A, Bruns OT, Reimer R, et al. Brown adipose tissue activity controls triglyceride clearance. Nat Med 2011;17:200–205
46. Beuckmann CT, Aoyagi M, Okazaki I, et al. Binding of biliverdin, bilirubin, and thyroid hormones to lipocalin-type prostaglandin D synthase. Biochemistry 1999;38:8006–8013